# Coded Spatial Modulation applied to Optical Wireless Communications in Indoor Environments

Thilo Fath*†, Jirka Klaue* and Harald Haas†

*EADS Innovation Works Germany
EADS Deutschland GmbH
81663 Munich, Germany
{thilo.fath, jirka.klaue}@eads.net

†Institute for Digital Communications
School of Engineering and Electronics
The University of Edinburgh
EH9 3JL, Edinburgh, UK
h.haas@ed.ac.uk

***Abstract*—Spatial Modulation (SM) is a combined multiple-input-multiple-output (MIMO) and digital modulation technique which besides common signal modulation conveys additional information bits in the spatial domain. To this end, only one transmitter is active at any time instance. The actual index of each emitter represents a unique spatial constellation point and thus conveys additional information. As a consequence, SM completely avoids inter-channel interference (ICI) and provides low detection complexity. Like for any MIMO scheme, the performance of SM is degraded in the presence of high channel correlation. Therefore, Trellis Coded Spatial Modulation (TCSM) applies coding techniques to the bits conveyed in the spatial domain to assist the detection of the active transmitter. As optical wireless communications (OWC) in indoor environments is subject to high spatial correlation and low channel distinctness, we evaluate the performance of coded SM applied to indoor OWC. For this purpose, we propose an enhanced coded SM technique which jointly encodes the bits conveyed in the signal and spatial domains. It is found in this paper that our enhanced coded SM technique can achieve gains in signal to noise ratio (SNR) of about $1-3$ dB compared to the originally proposed TCSM scheme.**

***Index Terms*—coding, MIMO, optical wireless communications, spatial modulation.**

## I. Introduction

Due to recent advances in solid-state lighting and the associated availability of frequency spectrum of hundreds of THz, optical wireless communications (OWC) has attracted attention for indoor data transmission as a promising complement to existing radio frequency (RF) systems [1]. Commonly for OWC, incoherent light sources are used as they enable the use of simple low cost optical devices. As a consequence, optical systems are mostly based on intensity modulation (IM) and direct detection (DD) by employing light emitting diodes (LEDs) as emitters and photo diodes as receivers, thus not providing phase information in the received signals [2]. Since there is an increasing adoption of LED lighting in homes and offices, this has fueled research that aims at using these devices not only for illumination but also for wireless communications [3]. Moreover, as there typically are several LEDs in an entire LED cluster, these multiple emitters can be used for data transmission. This inherently provides the essential prerequisite for the use of multiple-input-multiple-output (MIMO) techniques in conjunction with OWC [4]. MIMO techniques are already widely used in RF communications to enhance the system performance as they increase the link reliability and provide high data rates [5].

Recently, Spatial Modulation (SM) has been proposed as a combined MIMO and digital modulation technique [6]. In addition to applying basic signal modulation, SM transmits additional bits in the spatial domain by considering the transmitter array as an extended constellation diagram. As only one transmitter is emitting a digitally modulated signal at any time instance, the index of this transmitter represents additional data bits. It has been shown that SM can outperform other MIMO schemes like Repetition Coding (RC) [7] and spatial multiplexing [6], while even providing lower computational complexity.

Like for any MIMO technique, the performance of SM is related to the channel characteristics. As a consequence, its performance is degraded in scenarios with high link correlation and low channel distinctness. Therefore, Trellis Coded Spatial Modulation (TCSM) has been proposed to improve the performance of SM over correlated channels [8], [9]. TCSM applies coding to the bits conveyed in the transmitter index in order to increase the free distance between sequences of spatial constellation points. Consequently, the transmitter detection is made more robust and the error ratio is reduced. In order to achieve these gains, TCSM splits the data bits into two subsets. The first subset directly specifies the digitally modulated signal to be emitted, whereas the second subset is first passed to an encoder and then used to determine the emitter to be activated. Consequently, TCSM differentiates between the bits represented by digital signal modulation and the bits conveyed in the spatial domain. However, this approach disallows a joint decoding at the receiver side, thus not allowing the full exploitation of the SM principle.

Therefore, in this paper we extend the TCSM technique to an enhanced coded SM scheme which jointly encodes the bits conveyed in the spatial as well as in the signal domain. To this end, a convolutional encoder is applied to all data bits *before* they are split into the two subsets which determine the digitally modulated signal and the active transmitter. It is found that our jointly encoding achieves higher coding gains than the originally proposed TCSM scheme if applied to OWC.

The remainder of this paper is organised as follows: in Section II the basic system model is given. Section III introduces the setup which is used to model the optical wireless indoor scenario. Actual channel measurements substantiate the chosen model. In Section IV the bit error ratio (BER) performance of our proposed enhanced coded SM scheme is evaluated and compared to the original TCSM scheme [8], [9] as well as to uncoded SM. Finally, Section V concludes the paper.

## II. System Model

The considered system model comprises $N_t$ optical transmitters and $N_r$ receivers. The $N_r$-dimensional received signal vector is expressed as follows:

$$\mathbf{y} = \mathbf{H}\,\mathbf{s} + \mathbf{n} \quad \text{with} \quad \mathbf{y} \in \mathbb{R}^{N_r}, \tag{1}$$

where the transmitted signal vector is denoted by $\mathbf{s} = [s_1 \;\ldots\; s_{N_t}]^T$ with $[\cdot]^T$ being the transpose operator and $s_{n_t}$ depicting the signal emitted by transmitter $n_t$. The $N_r \times N_t$ channel matrix

$$\mathbf{H} = \begin{pmatrix} h_{11} & \cdots & h_{1N_t} \\ \vdots & \ddots & \vdots \\ h_{N_r 1} & \cdots & h_{N_r N_t} \end{pmatrix} \tag{2}$$

denotes the respective channel gain of the link between transmitter $n_t$ and receiver $n_r$. Moreover, $\mathbf{n}$ is the noise vector with $N_r$ elements, assumed to be real valued additive white Gaussian noise (AWGN) with zero mean, double-sided power spectral density $E_n$ and variance $\sigma^2$.

The basic principle of SM is that besides transmitting data by common signal modulation, *e.g.* amplitude modulation, it uses the transmitter index to convey additional bits. To this end, only one transmitter is emitting a signal at any time instance. Consequently, only one element of the signal vector $\mathbf{s}$ is non-zero and the index of this element represents the emitter to be activated. Fig. 1 illustrates the functionality of SM for a setup with $N_t = 4$ optical emitters and a signal constellation size of $M = 4$. As the spectral efficiency of SM is $\log_2(M\,N_t)$ bit/s/Hz, 4 bits can be transmitted per channel use in this example. The bits are passed to the SM mapper, which maps them to a signal constellation point and a transmitter index. As shown, the last two bits denote the index of the transmitter, whereas the first two bits represent the actual signal to be sent. For instance, the bit sequence "1 1 1 0" is represented by LED number 4 emitting signal $I_3$.

In the following, pulse amplitude modulation (PAM) is considered for signal modulation as it is widely used in OWC because of its simple implementation. The intensities which are used for the signal modulation of SM are given by

$$I_m = \frac{2\,I}{M+1}\,m \quad \text{for} \quad m = 1 \ldots M, \tag{3}$$

with $I$ denoting the mean optical intensity being emitted. Note that these intensities differ from common PAM as SM cannot operate with a signal intensity of $I_m = 0$. This is due to the fact that for $I_m = 0$, no emitter would be activated and the information conveyed in the spatial domain would be lost.

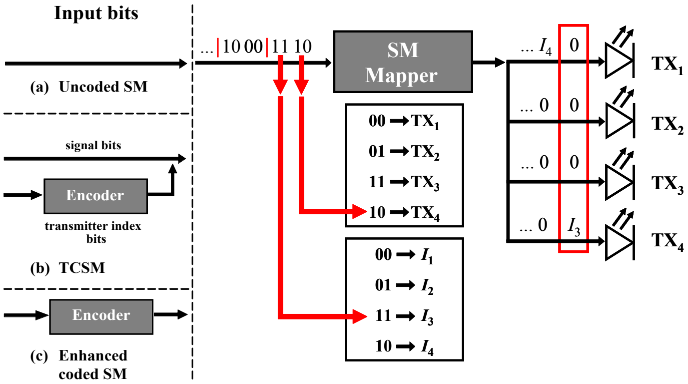


Fig. 1. Illustration of SM operation with $N_t = 4$ and $M = 4$.

The detection at the receiver side is based on the maximum-likelihood (ML) principle. Therefore, the detector decides for the constellation vector $\widehat{\mathbf{s}}$ which minimises the Euclidean distance between the actual received signal vector $\mathbf{y}$ and all potential received signals leading to

$$\widehat{\mathbf{s}} = \arg\max_{\mathbf{s}} p_{\mathbf{y}}(\mathbf{y}|\mathbf{s},\mathbf{H}) = \arg\min_{\mathbf{s}} \|\mathbf{y} - \mathbf{H}\,\mathbf{s}\|_{\mathrm{F}}^2\,, \tag{4}$$

where $\|\cdot\|_{\mathrm{F}}$ denotes the Frobenius norm and $p_{\mathbf{y}}$ is the probability density function of $\mathbf{y}$ conditioned on $\mathbf{s}$ and $\mathbf{H}$ with $p_{\mathbf{y}}(\mathbf{y}|\mathbf{s},\mathbf{H}) \propto \exp\left(-\|\mathbf{y} - \mathbf{H}\,\mathbf{s}\|_{\mathrm{F}}^2 / \sigma^2\right)$. Consequently, the ML detector jointly estimates the emitter index and the transmitted signal by a common operation. In the following it is assumed that the receiver has perfect knowledge of the channel, whereas $\mathbf{H}$ is not known at the transmitter side. If forward error correction (FEC) coding is applied, the ML detection principle given in (4) can be used to realise a soft decision ML detector for SM by employing log-likelihood ratios (LLRs). According to [10], the a posteriori LLR for the $i^{\text{th}}$ bit conveyed in the transmitted signal vector $\mathbf{s}$ is

$$L(\mathbf{s}^i) = \log \frac{\sum\limits_{\mathbf{s}\,\in\,\mathbf{S}_1^i} \exp\left(-\frac{\|\mathbf{y}-\mathbf{H}\,\mathbf{s}\|_{\mathrm{F}}^2}{\sigma^2}\right)}{\sum\limits_{\mathbf{s}\,\in\,\mathbf{S}_0^i} \exp\left(-\frac{\|\mathbf{y}-\mathbf{H}\,\mathbf{s}\|_{\mathrm{F}}^2}{\sigma^2}\right)}, \tag{5}$$

where $\mathbf{S}_1^i$ and $\mathbf{S}_0^i$ represent the set of signal vectors which have "1" and "0" at the $i^{\text{th}}$ bit position, respectively. The calculated LLRs can be processed by a soft decision Viterbi decoder in order to retrieve the transmitted data bits.

## III. Optical Wireless Setup

In this paper, intensity modulated optical wireless links with line-of-sight (LOS) characteristics are considered. According to [2], the channel gain of a directed LOS link can be determined using its geometric alignment yielding to

$$h = \begin{cases} \frac{(k+1)\,A\,r}{2\,\pi\,d^2} \cos^k(\phi)\cos(\psi) & 0 \le \psi \le \Psi_{\frac{1}{2}} \\ 0 & \psi > \Psi_{\frac{1}{2}} \end{cases} \tag{6}$$

where $\Psi_{\frac{1}{2}}$ is the field-of-view (FOV) semiangle of the receiver, $k = \frac{-\ln(2)}{\ln\left(\cos(\Phi_{\frac{1}{2}})\right)}$ and $\Phi_{\frac{1}{2}}$ is the transmitter semiangle (at half

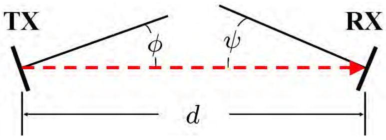


Fig. 2. Geometric scenario used for calculation of channel coefficients.

power). Moreover, $r$ denotes the optical-to-electrical conversion coefficient and $A$ is the detector area of the receiver. The distance between transmitter and receiver is depicted by $d$. As illustrated in Fig. 2, $\phi$ is the angle of emergence with respect to the transmitter (TX) axis and $\psi$ is the angle of incidence with respect to the receiver (RX) axis. Consequently, the channel gain $h_{n_r n_t}$ depends on the position of both transmitter $n_t$ and receiver $n_r$, *i.e.* their distance and angular alignment. Due to the use of SM, only one transmitter is emitting at any time instance and given independent identically distributed (i.i.d.) ones and zeros as data bits, each transmitter is activated with equal probability. Therefore, the average electrical power collected at each receiver is donated by $E_{\mathrm{RX}} = \left( \frac{1}{N_r} \frac{1}{N_t} \sum_{n_r=1}^{N_r} \sum_{n_t=1}^{N_t} h_{n_r n_t} I \right)^2$.

Without loss of generality, the performance of the evaluated SM schemes is studied using practical system parameters as follows: we analyse the channel gains of a setup which employs an off-the-shelf DL-6147-040 diode [11] at the transmitter side with $\Phi_{\frac{1}{2}} \approx 8°$ and a wavelength of 658 nm. The optical receiver consists of a circuitry applying a BPX 61 Silicon PIN (positive intrinsic negative) photo diode [12] with an optical-to-electrical conversion coefficient of $r \approx 0.434$ A/W at 658 nm, a detector area of $A \approx 7$ mm$^2$ and $\Psi_{\frac{1}{2}} \approx 55°$. The 3 dB cut-off frequency of the photo diode is about 17 MHz.

Fig. 3 displays an arbitrary optical wireless test setup which is used for channel measurements employing the diodes given above. As illustrated, the setup consists of two identical transmitters $\mathrm{TX}_1$ and $\mathrm{TX}_2$ which have a directed LOS connection towards the receiver. The spacing of the two transmitters is fixed to be 30 cm while their distance to the receiver $d_1$, respectively $d_2$, is varied. Both transmitters are oriented towards the receiver so that $\phi_1 = \phi_2 = 0$. As $\mathrm{TX}_1$ is directly placed on the receiver axis, $\psi_1 = 0$ holds. However, $\mathrm{TX}_2$ has an angular misalignment $\psi_2$ with respect to the receiver axis. Fig. 4 shows the measured channel gains for two scenarios,

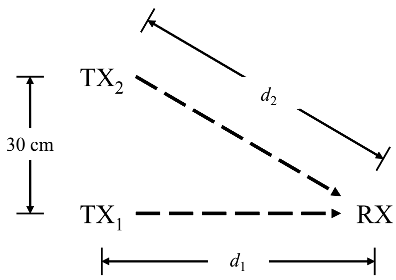


Fig. 3. Illustration of the optical wireless test setup.

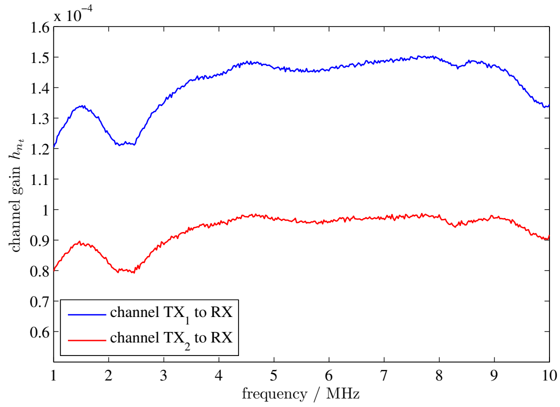


(a) channel gains for $d_1 = 50$ cm and $d_2 \approx 58$ cm.

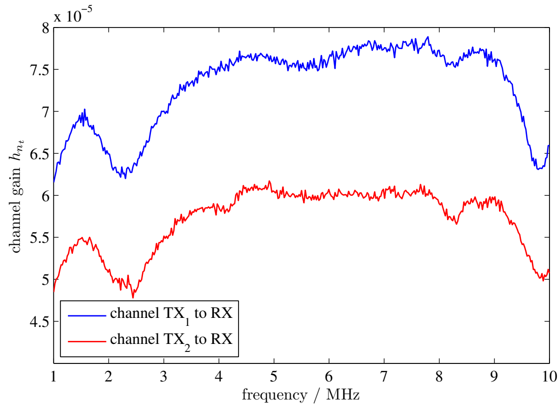


(b) channel gains for $d_1 = 70$ cm and $d_2 \approx 76$ cm.

Fig. 4. Measured gains of the optical wireless channels within the test setup.

similar to the setup presented in [13]. The gains are plotted for a frequency range of $1-10$ MHz. For scenario 4(a), $d_1 = 50$ cm, $d_2 \approx 58$ cm and $\psi_2 \approx 31°$. For scenario 4(b), $d_1 = 70$ cm, $d_2 \approx 76$ cm and $\psi_2 \approx 23°$. The measurements show that the links are highly correlated and differ only by their absolute gain, due to the larger distance and angular misalignment of $\mathrm{TX}_2$. Consequently, the gains have a time averaged correlation coefficient of

$$\rho(h_1, h_2) = \frac{\mathrm{E}\left\{(h_1 - \mathrm{E}\{h_1\})(h_2 - \mathrm{E}\{h_2\})\right\}}{\sqrt{\mathrm{VAR}\{h_1\}\,\mathrm{VAR}\{h_2\}}} \approx 0.97,$$

with $\mathrm{E}\{\cdot\}$ denoting the expectation operator and $\mathrm{VAR}\{\cdot\}$ being the variance operator. Moreover, the measured optical channels show only little variations within the considered frequency range as their maximum coefficient of variation, $v_n = \sqrt{\mathrm{VAR}\{h_n\}}/\mathrm{E}\{h_n\}$, is only about 0.07. Therefore, the links can be represented by flat AWGN channels with constant attenuation. Table I displays the mean measured channel gains $\overline{h_n}$ and the theoretical channel gains $h_n$ for scenario 4(a) and 4(b). Moreover, the relative difference, $\Delta_n = 100 \left|\overline{h_n} - h_n\right| / h_n$, between the measured gains and the theoretical values is given. As the maximum difference is only about 6.49 %, the measured channel gains and the gains calculated using the geometrical model closely match.

TABLE I
COMPARISON OF MEASURED AND THEORETICAL CHANNEL GAINS.

| | scenario 4(a) | scenario 4(b) |
|---|---|---|
| **theoretical gain** | $h_1 \approx 139.01\ 10^{-6}$<br>$h_2 \approx\ \ 87.65\ 10^{-6}$ | $h_1 \approx 70.93\ 10^{-6}$<br>$h_2 \approx 55.07\ 10^{-6}$ |
| **measured gain** | $\overline{h_1} \approx 141.59\ 10^{-6}$<br>$\overline{h_2} \approx\ \ 93.34\ 10^{-6}$ | $\overline{h_1} \approx 73.05\ 10^{-6}$<br>$\overline{h_2} \approx 57.17\ 10^{-6}$ |
| **relative difference** | $\Delta_1 \approx 1.86\ \%$<br>$\Delta_2 \approx 6.49\ \%$ | $\Delta_1 \approx 2.99\ \%$<br>$\Delta_2 \approx 3.81\ \%$ |

Therefore, we use this model in the following to derive the channel gains of different indoor setup scenarios. To this end, we consider a generic $4 \times 4$ indoor scenario ($N_r = 4$ and $N_t = 4$), which is located within a $4.0\,\text{m} \times 4.0\,\text{m} \times 3.0\,\text{m}$ room. We assume that the transmitters are placed at a height of $z = 3.00$ m and are oriented downwards to point straight down from the ceiling. The receivers are located at a height of $z = 0.75$ m (*e.g.* height of a table) and are oriented upwards to point straight up at the ceiling. Both transmitters and receivers are aligned in a quadratically $2 \times 2$ array which is centered in the middle of the room. On the basis of this scenario, we investigate different static setups with varying element spacings of the single transmitters on the $x$- and $y$-axis, depicted by $d_{\text{TX}}$, while the element spacing of the receivers is assumed to be $0.1$ m on the $x$- and $y$-axis for all considered setups. This receiver spacing is chosen with regard to a practical implementation within a potential (hand-held) user device. Fig. 5 exemplarily shows the positioning of the $4 \times 4$ setup, at which the receivers are displayed as dots and the transmitters as triangulars. The plotted cones illustrate the orientation of the transmit beams and the orientation of the receiver FOV. Applying (6) to this setup with $d_{\text{TX}} = 0.3$ m, $0.5$ m and $0.7$ m, results in the following channel matrices:

$$\mathbf{H}_{d_{\text{TX}}=0.3} \approx\ 10^{-5} \begin{pmatrix} 0.5934 & 0.4775 & 0.4775 & 0.3847 \\ 0.4775 & 0.5934 & 0.3847 & 0.4775 \\ 0.4775 & 0.3847 & 0.5934 & 0.4775 \\ 0.3847 & 0.4775 & 0.4775 & 0.5934 \end{pmatrix},$$

$$\mathbf{H}_{d_{\text{TX}}=0.5} \approx\ 10^{-5} \begin{pmatrix} 0.3847 & 0.2691 & 0.2691 & 0.1889 \\ 0.2691 & 0.3847 & 0.1889 & 0.2691 \\ 0.2691 & 0.1889 & 0.3847 & 0.2691 \\ 0.1889 & 0.2691 & 0.2691 & 0.3847 \end{pmatrix}, \tag{7}$$

$$\mathbf{H}_{d_{\text{TX}}=0.7} \approx\ 10^{-5} \begin{pmatrix} 0.1889 & 0.1157 & 0.1157 & 0.0713 \\ 0.1157 & 0.1889 & 0.0713 & 0.1157 \\ 0.1157 & 0.0713 & 0.1889 & 0.1157 \\ 0.0713 & 0.1157 & 0.1157 & 0.1889 \end{pmatrix}.$$

It can be seen that the symmetrical arrangement of the transmitters and receivers leads to equal channel gains for the wireless links with the same alignment, *e.g.* $h_{n_r n_t} = h_{n_t n_r}$. Moreover, if the spacing $d_{\text{TX}}$ between the transmitters is small, the gains are quite similar, whereas if $d_{\text{TX}}$ gets larger, the differences between the links increase due to the geometry of the setup scenario, *i.e.* the enlarged angular misalignment.

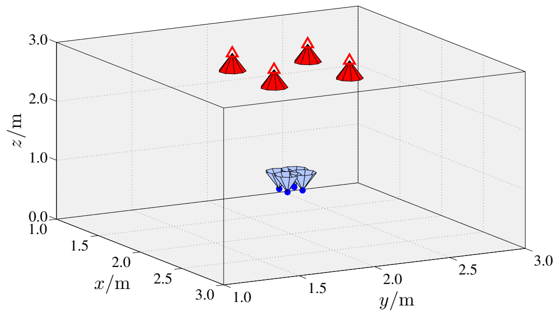

Fig. 5. Positioning of $4 \times 4$ setup with $d_{\text{TX}} = 0.5$ m within room.

## IV. Bit Error Ratio Performance of Coded Spatial Modulation

In the following, we evaluate the BER performance of coded SM applied to the optical wireless setup presented above. For encoding at the transmitter side, we assume a convolutional encoder with an octal presentation of $(161, 133)$, a coding rate of $c = \frac{1}{2}$, a constraint length of $l = 7$ and a free distance of $d_{\text{free}} = 10$. Furthermore, the encoded bits are additionally interleaved by a random block interleaver. As proposed in [8], [9], by applying TCSM, only the bits which determine the transmitter index are passed to the convolutional encoder, while the bits denoting the digitally modulated signal to be transmitted remain uncoded and are directly passed to the SM mapper (see Fig. 1 (b)). The encoded and interleaved bits are then used to determine the emitter which is activated according to the standard SM transmission scheme. In contrast, our proposed enhanced coded SM scheme passes *all* information bits to the convolutional encoder. The encoded bits are also interleaved and then passed to the standard SM mapper which maps them to the signal constellation points and transmitter indices as depicted in Fig. 1 (c). Note that for the sake of comparison, both coded SM schemes use the same $(161, 133)$ convolutional encoder. At the receiver side, the encoded bits of both coded SM schemes are deinterleaved and processed by a soft decision Viterbi decoder which has a traceback length of five times the constraint length.

Fig. 6 shows the BER performance of our enhanced coded SM scheme, TCSM and uncoded SM for a spectral efficiency of $R = 2$ bit/s/Hz in the considered $4 \times 4$ setup with different transmitter spacings of $d_{\text{TX}} = 0.3$ m, $0.5$ m and $0.7$ m. In order to provide this spectral efficiency, uncoded SM operates with a signal constellation size of $M = 1$, *i.e.* all bits to be transmitted are conveyed in the spatial domain because $R = \log_2(N_t)$. In contrast, TCSM has to operate with $M = 2$ to compensate for the redundancy induced by the encoder. Moreover, the enhanced coded SM scheme has to operate with an even larger constellation size of $M = 4$ to provide the same data rate. As shown, despite this enlarged signal constellation size, our enhanced coded SM scheme can achieve gains in signal to noise ratio (SNR) of about $2-3$ dB compared to TCSM and outperforms uncoded SM by about $6-10$ dB. Moreover, it can be seen that an enlargement of the transmitter spacing,

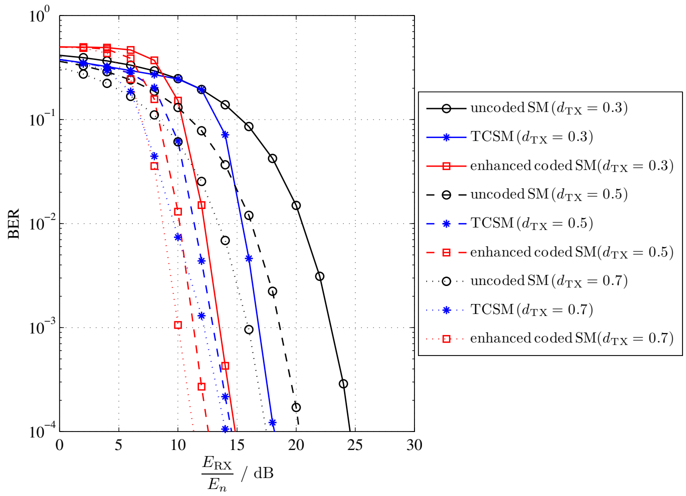


Fig. 6. BER of coded and uncoded SM for spectral efficiency of $R = 2$ bit/s/Hz in $4 \times 4$ setup scenario with varying distance $d_{\mathrm{TX}}$ of transmitters on the $x-$ and $y-$axis.

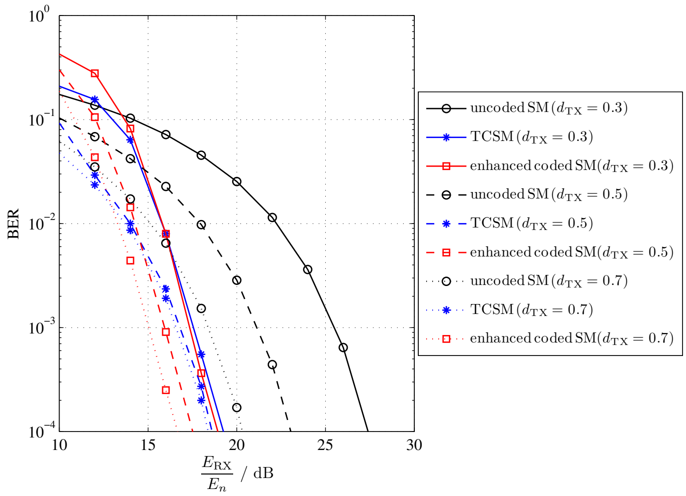


Fig. 7. BER of coded and uncoded SM for spectral efficiency of $R = 3$ bit/s/Hz in $4 \times 4$ setup scenario with varying distance $d_{\mathrm{TX}}$ of transmitters on the $x-$ and $y-$axis.

$d_{\mathrm{TX}}$, increases the channel distinctness and improves the BER performance of both coded and uncoded SM. Fig. 7 displays the BER of the considered schemes for $R = 3$ bit/s/Hz. In this scenario, uncoded SM operates with a signal constellation size of $M = 2$ and TCSM with $M = 4$. The enhanced coded SM scheme has to operate with $M = 16$. As depicted, the new enhanced coded SM scheme can also outperform both other schemes for $R = 3$ bit/s/Hz and achieves SNR gains of about $1 - 2$ dB compared to TCSM, respectively of about $4 - 8$ dB compared to uncoded SM, despite the fact that it has to use a much larger signal constellation size to compensate for the induced FEC coding.

## V. Summary and Conclusion

In this paper, we have studied the performance of coded SM applied to OWC in indoor environments. It has been shown that FEC coding can significantly improve the performance of SM under conditions with high link correlation and low channel distinctness. Moreover, we have proposed an enhanced coded SM scheme which jointly encodes the bits conveyed in the spatial and signal domains. It has been found in this paper that our approach can outperform the originally proposed TCSM scheme by several dB. This is because the jointly encoding conveys the coded bits in the spatial as well as in the signal domain. As a consequence, our enhanced coded SM scheme can make better use of the basic SM detection principle which jointly detects the emitter index and the transmitted signal by a common operation. Consequently, our enhanced coded SM scheme utilises the output of the ML detector more efficiently than the originally proposed TCSM scheme, thus providing larger coding gains. Future work might deal with the performance of coded SM for higher spectral efficiencies and different coding rates as well as its evaluation for outdoor free space optical (FSO) communications employing laser diodes.

## References


[1] R. J. Green, H. Joshi, M. D. Higgins, and M. S. Leeson, "Recent Developments in Indoor Optical Wireless," *IET Communications*, vol. 2, no. 1, pp. 3–10, Jan. 2008.

[2] J. M. Kahn and J. R. Barry, "Wireless Infrared Communications," *Proceedings of the IEEE*, vol. 85, no. 2, pp. 265–298, Feb. 1997.

[3] Y. Tanaka, T. Komine, S. Haruyama, and M. Nakagawa, "Indoor Visible Communication Utilizing Plural White LEDs as Lighting," in *Proceedings of the* $12^{th}$ *IEEE International Symposium on Personal, Indoor and Mobile Radio Communications*, vol. 2, San Diego, CA, USA, Sep. 30–Oct. 3, 2001, pp. 81–85.

[4] D. C. O'Brien, Q. Shabnam, Z. Sasha, and G. E. Faulkner, "Multiple Input Multiple Output Systems for Optical Wireless; Challenges and Possibilities," in *Proceedings of SPIE*, San Diego, California, USA, Aug. 15–17 2006.

[5] E. Telatar, "Capacity of Multi-Antenna Gaussian Channels," *European Transaction on Telecommunication*, vol. 10, no. 6, pp. 585–595, Nov. / Dec. 1999.

[6] R. Mesleh, H. Haas, C. W. Ahn, and S. Yun, "Spatial Modulation – A New Low Complexity Spectral Efficiency Enhancing Technique," in *IEEE International Conference on Communication and Networking in China (CHINACOM)*, Beijing, China, Oct. 25–27, 2006, pp. 1–5.

[7] T. Fath, H. Haas, M. Di Renzo, and R. Mesleh, "Spatial Modulation applied to Optical Wireless Communications in Indoor LOS Environments," in *Proc. of the IEEE Global Communications Conference*, Houston, Texas, USA, Dec. 5–9, 2011, pp. 3001–3005.

[8] R. Mesleh, I. Stefan, H. Haas, and P. Grant, "On the Performance of Trellis Coded Spatial Modulation," in *ITG International Workshop on Smart Antennas (WSA'09)*, Berlin, Germany, Feb. 16–19 2009.

[9] R. Mesleh, M. Di Renzo, H. Haas, and P. M. Grant, "Trellis Coded Spatial Modulation," *IEEE Trans. on Wireless Commun.*, vol. 9, no. 7, pp. 2349–2361, July 2010.

[10] S. U. Hwang, S. Jeon, S. Lee, and J. Seo, "Soft-Output ML Detector for Spatial Modulation OFDM Systems," *IEICE Electronics Express*, vol. 6, no. 19, pp. 1426–1431, Oct. 2009.

[11] Tottori SANYO Electric Co., Ltd., "Datasheet: RED LASER DIODE DL-6147-040," Retrieved Sep. 08, 2011 from http://combinlasers.com/1sanyo/dl-6147-040.pdf, May 2005.

[12] OSRAM Opto Semiconductors GmbH, "Datasheet: BPX 61 Silicon PIN Photodiode, Lead (Pb) Free Product - RoHS Compliant," Retrieved Sep. 08, 2011 from http://catalog.osram-os.com, Mar. 2007.

[13] T. Fath, M. Di Renzo, and H. Haas, "On the Performance of Space Shift Keying for Optical Wireless Communications," in *Proc. of the IEEE Global Communications Conference - Workshop on Optical Wireless Communications*, Miami, Florida, USA, Dec. 10, 2010, pp. 990–994.